

Cite this: *RSC Adv.*, 2017, 7, 43445

# Removal of Cd(II) and Pb(II) ions from natural water using a low-cost synthetic mineral: behavior and mechanisms

Gongning Chen<sup>ab</sup> and Lin Shi<sup>ID</sup>\*<sup>ab</sup>

A low-cost synthetic mineral (LCSM) was prepared by mechanochemical treatment of a solid-state mixture containing potassium feldspar, wollastonite, gypsum, limestone and dolomite powder at a molar ration of 1 : 1 : 1 : 6 : 3 and hydration process. The predominant activated mineralogical compositions of LCSM are gehlenite, montmorillonite and zeolites (laumontite and gismondine). The Cd(II) and Pb(II) ion removal behavior of LCSM from natural water was evaluated in batch mode as a function of contact time, pH, temperature, adsorbent dosage and concentration of initial metals. The results indicated that the adsorption process was pH dependent, endothermic and spontaneous. Meanwhile, the adsorption experiment data follows the Freundlich isotherm and the kinetic data best fit the pseudo-second order kinetic model. The maximum adsorption capacity obtained from the Freundlich isotherm at 25 °C was 32.8 mg g<sup>-1</sup> for Cd(II) and 268 mg g<sup>-1</sup> for Pb(II) ions, showing much higher removal capacity than the relevant previous studies. The metal ion removal by LCSM mainly occurs by an ion exchange mechanism, followed by precipitation and adsorption. Further, the adsorbed Cd(II) and Pb(II) on LCSM can hardly be desorbed at pH 3.0 and the desorption rates were even below 20% at pH 2.0, which indicates the excellent stability of LCSM and the heavy metals adsorbed are difficult to release into natural water. Therefore, despite its poor regenerability, LCSM can still be a good alternative adsorbent for removing metal ions from natural water or a soil amendment used for heavy metal immobilization when considering the abundance of low-cost raw materials used for its preparation, its good chemical stability and the amounts of mineral nutrients it contains.

Received 20th July 2017  
Accepted 4th September 2017

DOI: 10.1039/c7ra08018b

rsc.li/rsc-advances

## 1. Introduction

Toxic heavy metals such as cadmium and lead are nowadays environmental priority pollutants because of their characteristics of non-biodegradability, persistence and biological accumulation, which lead to public health hazards and environmental degradation.<sup>1,2</sup> Thus, a number of techniques have been employed generally for the elimination of metal ions from aquatic environments including chemical precipitation, solvent extraction, ion-exchange, reverse osmosis or adsorption *etc.*<sup>3–5</sup> Among them, ion exchange or adsorption by absorbents has been found to be superior compared to the other techniques for the treatment of natural water contaminated by heavy metals due to its advantages such as flexibility and simplicity of design, ease of operation, rapidness, effectiveness, suitability and environment-friendly nature.<sup>4–6</sup> However, the

removal of heavy metals from natural water by universal cation ion exchangers or adsorbents (*e.g.*, activated carbon, zeolite and montmorillonite) can be quite costly because of its extensive need.<sup>7,8</sup> Therefore, synthesis of some effective and environment-friendly adsorbents using low-cost raw materials for removing metals is a subject of considerable interest in recent years.

Mineral materials have been recognized as the “Green Material” in 21st century.<sup>9</sup> A number of low-cost and abundant minerals have been extensively used as adsorbents or raw material in the synthesis of effective adsorbents for heavy metal removal from natural water.<sup>5,10</sup> Previous study has shown that pure montmorillonite with Al and Mg in the octahedral sheet was synthesized in the MgO–Al<sub>2</sub>O<sub>3</sub>–SiO<sub>2</sub> systems at autogenously pressure.<sup>11</sup> Reyes and Fiallo found that illite was successfully transformed into highly crystalline faujasite-type zeolite by fusion with NaOH pellets at 600 °C followed by hydrothermal treatment.<sup>12</sup> Meanwhile, clay minerals such as montmorillonite and zeolite are capable of adsorbing heavy metals *via* cation exchange and formation of inner-sphere complexes through Si–O and Al–O groups.<sup>13</sup> Gehlenite has been reported to be prepared by solid-state reaction of mechanochemically treated mixtures of kaolinite, calcite and aluminum hydroxide at 900 °C, also showed high absorption

<sup>a</sup>School of Environment and Energy, South China University of Technology, Guangzhou Higher Education Mega Centre, Guangzhou, PR China. E-mail: celshi@126.com; Fax: +86 2085511266; Tel: +86 2033757292

<sup>b</sup>The Key Lab of Pollution Control and Ecosystem Restoration in Industry Clusters, Ministry of Education, South China University of Technology, Guangzhou Higher Education Mega Centre, Guangzhou, PR China



capacity for metal ions.<sup>10</sup> In order to synthesize the above three effective adsorbents by calcination in the CaO–MgO–SiO<sub>2</sub>–Al<sub>2</sub>O<sub>3</sub> system, some low cost and abundant mineral materials such as potassium feldspar and wollastonite in this study were elected as silicon and aluminum source, limestone and dolomite were used to provide some smaller radius of cations such as Ca<sup>2+</sup> and Mg<sup>2+</sup> in order to displace K<sup>+</sup> in the crystal structure of potassium feldspar, which contributes to higher CEC. The replaced K<sup>+</sup> can be fixed by anions with high electronegativity such as SO<sub>4</sub><sup>2-</sup> in gypsum. Moreover, the reaction temperature can also be decreased due to the addition of gypsum.<sup>14</sup> In addition, this synthetic mineral is rich in available K, Ca, Mg and Si, which are essential cations for soil and crops growth.<sup>15</sup> Therefore, this technology will be a kind of environmental protective high-efficiency new technology of utilizing mining resources.

In the context of the above, low-cost synthetic mineral (LCSM) in this study was prepared by mechanochemical treatments of a solid-state mixture of potassium feldspar, wollastonite, gypsum, limestone and dolomite and hydration process. Batch experiments were performed to evaluate the influences of various experimental parameters such as contact time, pH, temperature, adsorbent dosage and initial Cd(II) and Pb(II) concentration on the adsorption of Cd(II) and Pb(II) from aqueous solution. And the kinetics, equilibrium and thermodynamic data of the adsorption process were studied to understand the adsorption behaviors. Finally, the mechanism responsible for heavy metal removal by LCSM was discussed in detail.

## 2. Materials and methods

### 2.1. Chemicals and materials

The potassium feldspar was derived from Shandong Province, PR China. The wollastonite, dolomite, gypsum and limestone were procured from Antu County, Jilin Province, PR China. All these raw materials were pulverized by ball milling then passed through a 200 meshes sieve (about 74 µm in diameter). All other chemicals used in this study were of analytical grade. Stock solution of Pb<sup>2+</sup> (2000 mg L<sup>-1</sup>) and Cd<sup>2+</sup> (1000 mg L<sup>-1</sup>) were prepared by separately dissolving appropriate quantity of analytical grade Pb(NO<sub>3</sub>)<sub>2</sub> and Cd(NO<sub>3</sub>)<sub>2</sub> without further purification, and other concentrations were prepared from the stock solution by dilution.

### 2.2. Instrumentation and techniques

The mineralogical compositions of LCSM were determined by the X-ray Diffraction (XRD) analysis using an automated diffractometer (DeMax III, Rigaku, Japan) having a Ni filtered Cu Kα radiation. The chemical composition of the LCSM was determined by an X-ray fluorescence (XRF) spectrometer (Axios Pw4400, PANalytical, Netherlands). The microstructure before and after metal ions adsorption was investigated by Scanning Electron Microscope (SEM) (EVO 40, Carl Zeiss AG, USA) of selected samples. Particle size of LCSM was measured by Malvern Hydro 2000S Master Size, Malvern Instruments Ltd., U.K. The specific surface area of LCSM was determined from the N<sub>2</sub>

gas adsorption isotherm at 77 K using a specific surface area analyzer (Autosorb-1-C/MS, Quantachrome, USA). The elemental composition of LCSM was determined using an X-ray photoelectron spectroscopy (XPS) spectrometer (Axis Ultra DLD-600W, Kratos, UK). The simultaneous Thermogravimetry (TG) and Differential Scanning Calorimetry (DSC) in the temperature range from 25 °C to 1000 °C were conducted on STA449C, Netzsch, Germany. Its heating atmosphere was air and the heating rate was 10 °C min<sup>-1</sup>. The pH value of LCSM was measured using PHS-25 type digital pH meter at a water/solid ratio of 50 : 1. The cation exchange capacity (CEC) was measured using the copper complex method<sup>16</sup> for which 0.6 mg of the sample was suspended for 12 h in 25 mL of a 0.01 M ethylene di-amine copper complex (Cu(EDA)<sub>2</sub>Cl<sub>2</sub>) solution. The mixture was centrifuged and the filtrates was analyzed for the Cu levels by graphite furnace atomic absorption spectrometry (Shimadzu, AA6300C, Japan). 0.2 g of the LCSM was added into a conical flask containing 40 mL of 2% citric acid solution and water, respectively. Subsequently, the conical flask was agitated at 220 rpm on a rotary shaker for 30 min, filtered and the citrate or water-soluble SiO<sub>2</sub> in the filtrates was measured by visible spectrophotometer.

### 2.3. Preparation of adsorbent

All raw materials such as potassium feldspar, wollastonite, gypsum, limestone and dolomite powder were weighed based on a molar ratio of 1 : 1 : 1 : 6 : 3, and added into a blended jar. After that, the blended powders were mixed with about 40% w/w water and ball milled for 2 h to allow adequate stirring, drying and calcination for 1 h at a temperature of 1000 °C into muffle furnace. Then, the reacted solid phase after cooling was pulverized and full hydrated with immersion treatment, followed by drying and grounded to 200 meshes. The obtained product was used as a low-cost synthetic mineral (LCSM) for further characterization and adsorption experiment.

### 2.4. Adsorption experiment

The adsorption behavior of Pb(II) and Cd(II) ions onto LCSM was performed in 50 mL polyethylene centrifuge tubes by batch equilibrium method. In a typical experiment, necessary amount of LCSM was added into each polyethylene centrifuge tubes containing 40 mL of Pb(II) and Cd(II) with appropriate concentrations. The solution pH was adjusted by adding drops of 0.1 M HNO<sub>3</sub> and 0.1 M NaOH to a desired pH value when necessary. Subsequently, the contents of the tube was agitated at 220 rpm on a rotary shaker for a desired time, filtered and quantitative analysis of remaining metal concentration in solution using graphite furnace atomic absorption spectrometry (GFAAS). The amount of removed heavy metal was calculated from the difference between initial and final concentration. Throughout the study, the pH ranges were 1–8 for Cd(II) and 1–7 for Pb(II), and the adsorbent dosage ranges were 2–12 g L<sup>-1</sup> for Cd(II) and 0.25–11 g L<sup>-1</sup> for Pb(II). All experiments were run in triplicate and the standard deviation was found to be within ±3%.

**Adsorption kinetics experiments.** Different tubes were treated following the general procedure described above and



samples were taken at predetermined time intervals ranging from 5 to 120 min at 25 °C. The initial Cd(II) concentration was 40 mg L<sup>-1</sup> with pH 4 and Pb(II) concentration was 350 mg L<sup>-1</sup> with pH 3. The dosage of LCSM was 5 g L<sup>-1</sup> and 3 g L<sup>-1</sup> for Cd(II) and Pb(II), respectively.

**Adsorption isotherms and thermodynamic experiments.** The initial Cd(II) concentration was varied from 40–400 mg L<sup>-1</sup> with pH 4 and Pb(II) concentration from 350–1500 mg L<sup>-1</sup> with pH 3. The dosage of LCSM was 5 g L<sup>-1</sup> and 3 g L<sup>-1</sup> for Cd(II) and Pb(II), respectively. The effect of temperature on adsorption isotherm was conducted under isothermal condition at 25–55 °C and the contact time was 30 min.

## 2.5. Desorption experiment

Desorption experiment were performed in an identical manner to the adsorption experiment. After the adsorption experiments, the metal-loaded LCSM was mixed with 40 mL of HNO<sub>3</sub> solution at pH 3.0, 2.0, 1.0 and 0.5, respectively. The mixtures were agitated at a speed of 220 rpm on a rotary shaker operating at 25 °C for 30 min, and then were centrifuged at 4000 rpm for 10 min. The mixtures were filtered out and analyzed for its metal ion concentrations using GFAAS. The desorption ratio was calculated from the amount of metal ions adsorbed on the LCSM and the final metal ions concentration in the elutriant.

# 3. Results and discussion

## 3.1. Physicochemical properties of adsorbent LCSM

The physicochemical properties of LCSM are also listed in Table 1. LCSM was found to be white and loose powder with an average particle diameter of 20.3 μm and slightly alkaline nature. The pH and CEC of LCSM was found to be 10.5 and 91.9 cmol kg<sup>-1</sup>, respectively. The main chemical composition of LCSM, determined using XRF, was 31.5% CaO, 30.4% SiO<sub>2</sub>, 4.99% SO<sub>3</sub>, 9.84% Al<sub>2</sub>O<sub>3</sub>, 4.77% MgO, 3.92% K<sub>2</sub>O. The high contents of SiO<sub>2</sub>, Al<sub>2</sub>O<sub>3</sub> and CaO would contribute to high removal of metals due to the presence silanol sites (≡Si-OH) and aluminols (≡Al-OH) groups at the surface of LCSM.<sup>17</sup> The water-soluble and citrate-soluble SiO<sub>2</sub> in LCSM was up to 0.66% and 19.8%, respectively, which could remove heavy metal ions from natural water by the formation of silicate precipitate.<sup>18</sup> The

presence of activated minerals in LCSM was confirmed through mineralogical composition by XRD analysis (Fig. 1(A)). A distinctive peak at 6.86, 9.32, 17.8, 16.2 and 21.0 2θ indicated the presence of montmorillonite, laumontite and gismondine, respectively. Similarly, the peaks at 11.7, 26.7, 29.0, 27.3, 33.3 and 47.5 2θ were characteristic peak of gypsum, microcline and grossular, respectively. Moreover, a distinctive peak at 23.1, 29.3, 53.2, 31.2, 44.4 and 52.1 2θ indicated the presence of calcium silicate and gehlenite, respectively. The nitrogen adsorption-desorption data and the pore size distribution for LCSM are presented in Fig. 1(B). It is apparent that the adsorption isotherms, which are obtained as the adsorption amount of gas enhanced with increasing relative pressure, are of type II according to the Brunauer, Deming, Deming and Teller (BDDT) classification.<sup>19</sup> The adsorption-desorption isotherms are overlapped at the low relative pressure region ( $P/P_0 \leq 0.40$ ) reveals the existence of some microspores.<sup>20</sup> This result in a H3-type hysteresis loop due to the LCSM comprising lumps and aggregates forming some small pores indicates the mesopores structure of the adsorbent.<sup>21</sup> The BET surface area, pore volume and average pore diameter of LCSM was 24.4 m<sup>2</sup> g<sup>-1</sup>, 0.046 cm<sup>3</sup> g<sup>-1</sup> and 7.55 nm, respectively.

To investigate the thermal activation process of LCSM, TG-DSC test was conducted and the result is presented in Fig. 2. The TG curve appeared a slight downtrend in the temperature range of 25–105 °C, which attributed to free water evaporation at about 103 °C, and then dehydration of CaSO<sub>4</sub>·2H<sub>2</sub>O forming CaSO<sub>4</sub>·1/2H<sub>2</sub>O, also known as calcined gypsum, in the temperature range of 109–130 °C, and finally completely losing all crystal water to form II-type CaSO<sub>4</sub> at above 163 °C. CaCO<sub>3</sub> and MgCO<sub>3</sub> should be theoretically decomposed into CaO, MgO and CO<sub>2</sub> at 825 °C and 790 °C, respectively. In the temperature range of 600–750 °C, nevertheless, a sharp fall occurred in the TG curve with a total material weight loss of about 17.5%, which implied that MgCO<sub>3</sub> and CaCO<sub>3</sub> were successively decomposed into MgO, CaO and CO<sub>2</sub> (eqn (1) and (2)) at a lower temperature (about 733 °C) with an endothermic reaction shown in DSC curve, which may attributed to CaSO<sub>4</sub> that helps to decrease the decomposing temperature.<sup>14</sup> Consequently, the activation reaction occurred at 1000 °C by calcining the mixture of all raw materials, resulting in the precursor of LCSM.

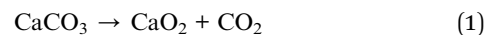


**Table 1** Relevant composition and physicochemical properties of the LCSM used in this study

Main chemical composition (%)		Physicochemical properties	
CaO	31.5	pH	10.5
SiO <sub>2</sub>	30.4	CEC <sup>a</sup> (cmol kg <sup>-1</sup> )	91.9
SO <sub>3</sub>	4.99	Particle diameter (μm)	20.3
Al <sub>2</sub> O <sub>3</sub>	9.84	BET surface area (m <sup>2</sup> g <sup>-1</sup> )	24.4
MgO	4.77	Pore volume (cm <sup>3</sup> g <sup>-1</sup> )	0.046
K <sub>2</sub> O	3.92	Water-soluble SiO <sub>2</sub> (%)	0.66
		Citrate-soluble SiO <sub>2</sub> (%)	19.8

<sup>a</sup> Cation exchange capacity.

The decomposition of K-feldspar at 1000 °C can be described by eqn (3). K-feldspar decomposed into KAlSi<sub>2</sub>O<sub>6</sub>, K<sub>2</sub>Al<sub>2</sub>SiO<sub>6</sub>, KAlSiO<sub>4</sub> and SiO<sub>2</sub>, and the equilibrium shifts to the right due to substantial consumption of SiO<sub>2</sub> by CaO (eqn (4)). The formation of Ca<sub>4</sub>(AlSi<sub>2</sub>O<sub>6</sub>)<sub>8</sub>, Ca<sub>2</sub>Al(AlSiO<sub>7</sub>), CaAl<sub>2</sub>Si<sub>2</sub>O<sub>8</sub> and Ca<sub>3</sub>Al<sub>2</sub>(SiO<sub>4</sub>)<sub>3</sub> can be described by eqn (5)–(8). In addition, potassium feldspar is the precursor of illite, and illite is similar to that of montmorillonite except the excess charges of Al are satisfied by K<sup>+</sup> between the silica sheets. During activation, sufficient amount of the K<sup>+</sup> could be removed from the precursor and



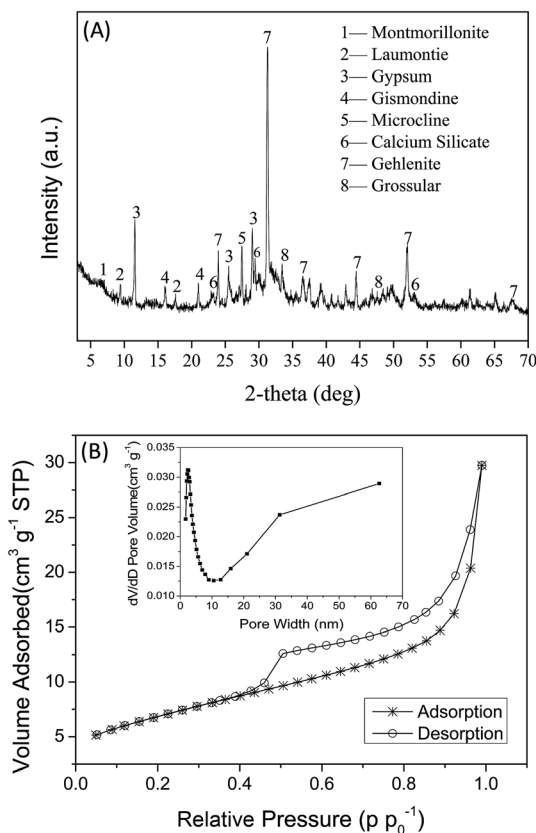


Fig. 1 X-ray diffraction patterns (A) and nitrogen adsorption-desorption isotherm and pore size/pore volume (inset) (B) of LCSM (low-cost synthetic mineral). Montmorillonite: (Na,Ca)<sub>0.33</sub>(Al,Mg)<sub>2</sub>(Si<sub>4</sub>-O<sub>10</sub>)(OH)<sub>2</sub>·4H<sub>2</sub>O; laumontite: Ca<sub>4</sub>(AlSi<sub>2</sub>O<sub>6</sub>)<sub>8</sub>·16H<sub>2</sub>O; gypsum: CaSO<sub>4</sub>·2H<sub>2</sub>O; gismondine: CaAl<sub>2</sub>Si<sub>2</sub>O<sub>8</sub>·4(H<sub>2</sub>O); microcline: KAlSi<sub>3</sub>O<sub>8</sub>; calcium silicate: 2CaO·SiO<sub>2</sub>; gehlenite: Ca<sub>2</sub>Al(AlSiO<sub>7</sub>); grossular: Ca<sub>3</sub>Al<sub>2</sub>(SiO<sub>4</sub>)<sub>3</sub>.

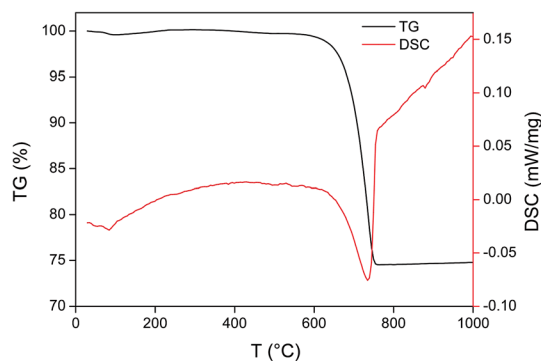
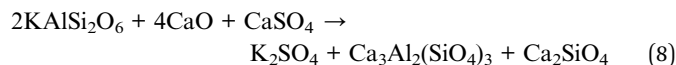
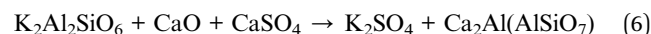


Fig. 2 TG-DSC curve in the thermal activation process of LCSM.

replaced by exchangeable Ca<sup>2+</sup> and Mg<sup>2+</sup>, which was structurally equivalent to a member of the montmorillonite. Meanwhile, it was evident that potassium was transformed to soluble sulfate forms, which plays an important role in the supplement of essential cations in soil and crops.<sup>15</sup>



### 3.2. Effect of pH

The influence of solution pH on the removal of Cd(II) and Pb(II) ions using LCSM was studied and the results are presented in Fig. 3. It was obvious that the removal of LCSM for both metal ions was highly pH dependent and more than 49% of Cd(II) and 86% of Pb(II) was removed at pH 2.0, which exhibited highly efficient removal even at strongly acidic conditions. The maximum removal efficiency was 99.4% for Cd(II) and 98.7% for Pb(II) ions, which was found to be at pH 4.0 and 3.0, respectively. The observed greater uptakes at higher pH were attribute to the fact that the available adsorption sites increases remarkably and the competition between H<sup>+</sup> and metal ions for the solid activated sites reduces significantly with increasing pHs.<sup>18</sup> Meanwhile, the negative charge on the LCSM surface increases and hence the electrostatic attraction between LCSM and metal ions becomes more strongly, thus, facilitating higher metal ions uptake.<sup>22</sup> Experiments were not carried out beyond pH 8.0 for Cd(II) and pH 7.0 for Pb(II) to avoid the formation of metal hydroxide precipitates. Therefore, the optimum pH for Cd(II) and Pb(II) removal was selected as 4.0 and 3.0, respectively.

### 3.3. Effect of LCSM dosage

The effect of LCSM dosage on the removal rate of Cd(II) and Pb(II) ions was investigated and the results are shown in Fig. 4. It

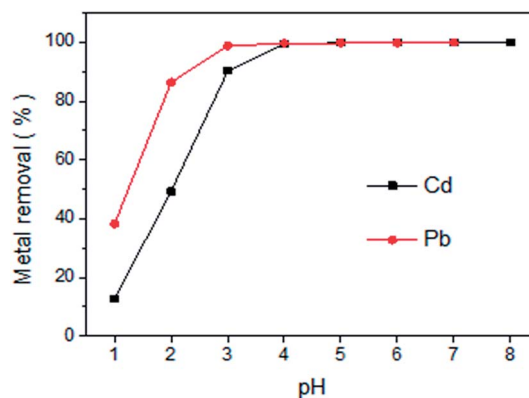


Fig. 3 Effect of pH on the adsorption of Cd(II) and Pb(II) onto LCSM (reaction conditions: Cd(II) concentration of 40 mg L<sup>-1</sup> with LCSM dosage of 5 g L<sup>-1</sup>; Pb(II) concentration of 350 mg L<sup>-1</sup> with LCSM dosage of 3 g L<sup>-1</sup>; 25 °C reaction temperature and 30 min of contact time).





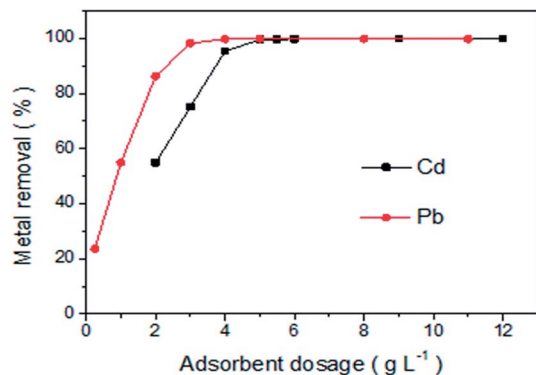


Fig. 4 Effect of adsorbent (LCSM) dosage on the adsorption of Cd(II) and Pb(II) (reaction conditions: Cd(II) concentration of  $40 \text{ mg L}^{-1}$  with pH 4 and Pb(II) concentration of  $350 \text{ mg L}^{-1}$  with pH 3;  $25^\circ\text{C}$  reaction temperature and 30 min of contact time).

was apparent that the removal performance of both metal ions increased sharply with LCSM dose. The percentage of Cd(II) removal increased from 54.9% to 99.5% with increasing the LCSM dosage from  $2.0$  to  $5.0 \text{ g L}^{-1}$ . Also, Pb(II) removal increased from 23.5% to 98.3% with increasing the LCSM dosage from  $0.25$  to  $3.0 \text{ g L}^{-1}$ . This observed trend was attributed to the increased numbers of vacant adsorption sites, enhanced distribution coefficient and more available surface area.<sup>18</sup> However, the removal rates become nearly constant when the LCSM dosage exceeds  $5.0 \text{ g L}^{-1}$  for Cd(II) and  $3.0 \text{ g L}^{-1}$  for Pb(II). The result could be due to the interference between binding sites at larger adsorbent amount or insufficiency of metal ions with more effective binding sites.<sup>23</sup>

#### 3.4. Effect of contact time and adsorption kinetics

The effects of contact time on metal ions removal are shown in Fig. 5(A), showing that the amount of metal ions adsorbed increased considerably with time. The removal rates of Cd(II) and Pb(II) by LCSM were rapid because adsorbates–adsorbent interactions reached equilibrium within 30 min and the removal rate reached about 98%. The rapid initial uptake is probably due to the abundant availability of adsorption sites

and the higher concentration gradient that drives fast diffusion of metal ions from solution to the external surface of LCSM.<sup>24</sup> However, the further uptake rate dropped gradually due to the limitation of available sites for occupation and the increase electrostatic repulsion between incoming metal ions and adsorbed metal ions. Thus, the contact time of 30 min was selected in the further adsorption experiments.

Two kinetic models namely pseudo-first-order and pseudo-second-order models were used to simulate the experimental data. For the pseudo-first order model,  $k_1$  and  $Q_{e \text{ cal}}$  can be determined from the slope and intercept of the linear plot of  $\ln(Q_e - Q_t)$  versus  $t$ , respectively. For the pseudo-second order model,  $k_2$  and  $Q_{e \text{ cal}}$  values were obtained from the intercept and slope of the plot of  $t/Q_t$  versus  $t$  (Fig. 5(B)). The comparison between the two kinetic models is presented in Table 2. The theoretical  $Q_{e \text{ cal}}$  values calculated by the pseudo-second order model were found to be closer to the experimental  $Q_{e \text{ exp}}$  values and the correlation coefficients were higher for both metal ions. Therefore, the second-order kinetics model can better describe the adsorption of Cd(II) and Pb(II) ions onto LCSM.

#### 3.5. Effect of concentration and adsorption isotherms

To explore the influences of initial metal ions concentration and temperature on the removal performance, the adsorption isotherms of Cd(II) and Pb(II) onto LCSM obtained at four different temperatures ( $25$ ,  $35$ ,  $45$  and  $55^\circ\text{C}$ ) are illustrated in Fig. 6. It was apparent that the amount of metal ions adsorbed enhanced with the increase of metal ions concentration until an equilibrium value is achieved. In order to elucidate the removal mechanism, three adsorption isotherms models namely Langmuir, Freundlich and Dubinin–Astakhov (D–A) isotherms models were plotted to fit the experimental data and accordingly calculated parameters are summarized in Table 3. It can be seen from the regression coefficient ( $R^2$ ) values presented in Table 3 that the adsorption isotherms models can well fit the adsorption equilibrium data in the following order: Freundlich ( $0.988 < R^2 < 0.998$ ) > D–A ( $0.941 < R^2 < 0.988$ ) > Langmuir ( $0.828 < R^2 < 0.906$ ). Thus, it can be concluded that Cd(II) and Pb(II) adsorption onto LCSM can be determined for multilayer adsorption processes and the surface of LCSM consist of small

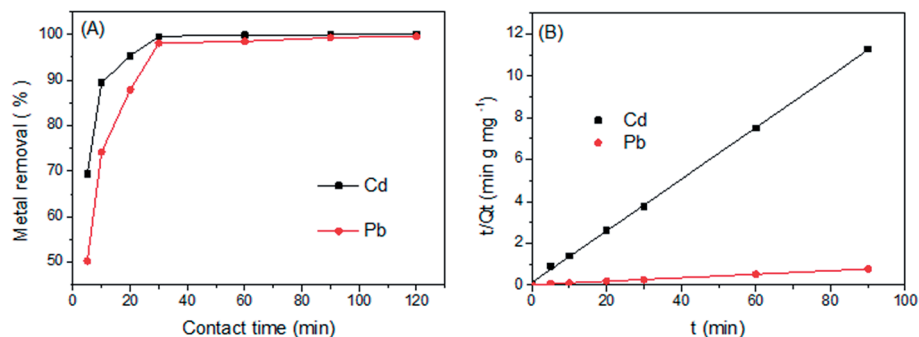


Fig. 5 Effect of contact time on the adsorption of Cd(II) and Pb(II) onto LCSM (A) and its pseudo-second-order kinetic plots (B) (reaction conditions: Cd(II) concentration of  $40 \text{ mg L}^{-1}$  with pH 4 and Pb(II) concentration of  $350 \text{ mg L}^{-1}$  with pH 3; LCSM dosage of  $5$  and  $3 \text{ g L}^{-1}$  for Cd(II) and Pb(II), respectively;  $25^\circ\text{C}$  reaction temperature).



Table 2 Kinetic parameters of pseudo-first-order and pseudo-second-order models<sup>a</sup>

Metals	$Q_e \text{ exp (mg g}^{-1}\text{)}$	Pseudo-first order kinetic model $\lg(Q_e - Q_t) = \lg Q_e - k_1 t/2.303$			Pseudo-second order kinetic model $\frac{t}{Q_t} = \frac{1}{k_2 Q_e^2} + \frac{1}{Q_e} t$		
		$k_1 \text{ (min}^{-1}\text{)}$	$Q_e \text{ cal (mg g}^{-1}\text{)}$	$R^2$	$k_2 \text{ (g mg}^{-1} \text{ min}^{-1}\text{)}$	$Q_e \text{ cal (mg g}^{-1}\text{)}$	$R^2$
Cd(II)	8.0	0.113	3.34	0.965	0.114	8.13	0.999
Pb(II)	116.2	0.060	53.6	0.877	0.003	125.0	0.997

<sup>a</sup>  $Q_e \text{ (mg g}^{-1}\text{)}$  and  $Q_t \text{ (mg g}^{-1}\text{)}$  are the amounts of the metal ions adsorbed onto LCSM at equilibrium and at any time ( $t$ ),  $k_1 \text{ (L min}^{-1}\text{)}$  and  $k_2 \text{ (g mg}^{-1} \text{ min}^{-1}\text{)}$  are the rate constants of the first and second order models, respectively.

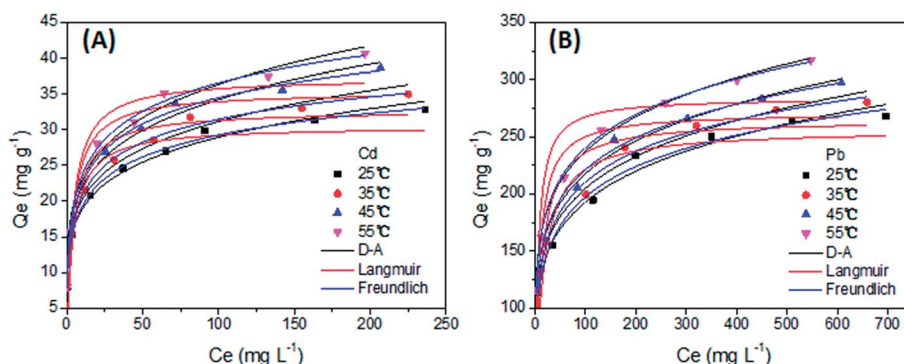


Fig. 6 Adsorption equilibrium curve of Cd(II) (A) and Pb(II) (B) on LCSM at different temperatures (reaction conditions: pH 4.0 for Cd(II) and 3.0 for Pb(II); LCSM dosage of 5 and 3 g L<sup>-1</sup> for Cd(II) and Pb(II), respectively; 30 min of contact time and a reaction temperature range of 25–55 °C).

heterogeneous particles.<sup>25</sup> The  $n$  values obtained from the Freundlich isotherm are greater than 1, showing that the adsorption of both metal ions is favorable. The value of  $E$  can be served to distinguish the type of removal mechanism, physical ( $E < 8 \text{ kJ mol}^{-1}$ ) or chemical ( $8 \text{ kJ mol}^{-1} < E < 16 \text{ kJ mol}^{-1}$ ).<sup>26</sup> As seen from Table 3, the  $E$  values for Cd(II) ions at different temperatures lie within 8–16 kJ mol<sup>-1</sup>, which shown that ion-exchange was the principal Cd(II) ions removal mechanism. The  $E$  values for Pb(II) ions removal were found to exceeded

16 kJ mol<sup>-1</sup>, which attributed to different chemical processes accompanying the ion exchange process.

The maximum removal capacity ( $Q_0$ ) of Cd(II) and Pb(II) ions obtained from the Freundlich models was increased with increasing temperature, which was within 32.8–40.7 mg g<sup>-1</sup> and 268.0–317.5 mg g<sup>-1</sup>, respectively. The different removal capacity between Cd(II) and Pb(II) could be attributed to their different affinities to LCSM. As noted from Table 4, The maximum Cd(II) and Pb(II) ions removal capacity of LCSM was rather higher than

Table 3 Adsorption isotherm parameters for the adsorption of Cd(II) and Pb(II) on LCSM at different temperatures<sup>a</sup>

Metal ions	Temperature (°C)	Freundlich isotherm $\frac{1}{Q_e} = \frac{1}{Q_0} + \frac{1}{bQ_0} \frac{1}{C_e}$			Langmuir isotherm $\log Q_e = \log K_f + \frac{1}{n} \log C_e$			D-A isotherm $\ln Q_e = \ln Q_0 - \left(\frac{1}{\sqrt{2}E}\right)^N \left[RT \ln \left(1 + \frac{1}{C_e}\right)\right]^N$			
		$K_f \text{ (mg g}^{-1}\text{)}/\text{(mg L}^{-1}\text{)}^{1/n}$	$n$	$R^2$	$Q_0 \text{ (mg g}^{-1}\text{)}$	$b \text{ (L mg}^{-1}\text{)}$	$R^2$	$Q_0 \text{ (mg g}^{-1}\text{)}$	$N$	$E \text{ kJ mol}^{-1}$	$R^2$
Cd(II)	25	11.48	4.93	0.992	25.6	2.29	0.906	88.3	0.146	8.8	0.969
	35	12.16	4.83	0.991	26.3	2.71	0.899	92.7	0.150	10.7	0.957
	45	13.06	4.69	0.993	27.8	3.60	0.893	99.8	0.155	12.6	0.963
	55	13.65	3.85	0.993	28.6	3.89	0.893	102.7	0.160	15.8	0.941
Pb(II)	25	78.16	5.13	0.989	235.9	0.12	0.871	484.9	0.193	31.5	0.983
	35	84.14	5.21	0.988	246.3	0.14	0.901	501.6	0.206	38.6	0.987
	45	93.11	5.46	0.992	251.3	0.22	0.890	528.4	0.210	43.4	0.988
	55	105.9	5.75	0.998	253.8	0.38	0.828	550.8	0.214	48.2	0.984

<sup>a</sup>  $Q_e \text{ (mg g}^{-1}\text{)}$  is the amount of mental ions adsorbed at equilibrium, and  $C_e \text{ (mg L}^{-1}\text{)}$  is concentration at equilibrium.  $Q_0 \text{ (mg g}^{-1}\text{)}$  and  $b \text{ (L g}^{-1}\text{)}$  are Langmuir isotherm parameters.  $K_f$  is a constant relating the adsorption capacity and  $n$  is an empirical parameter relating the adsorption intensity.  $T$  (K) is the temperature and  $R$  (8.314 J mol<sup>-1</sup> K<sup>-1</sup>) is the gas constant.  $E \text{ (kJ mol}^{-1}\text{)}$  is the adsorption energy and  $N$  is the heterogeneity parameter.



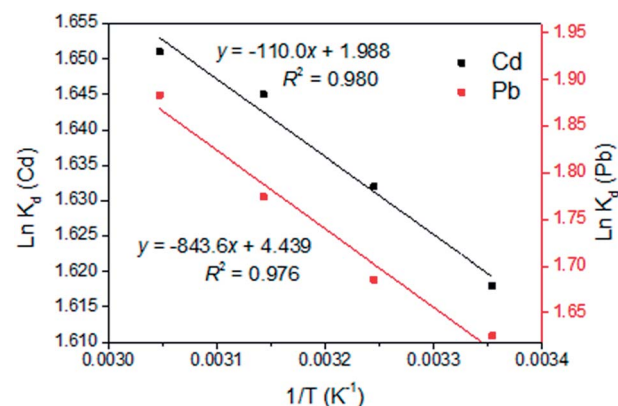
**Table 4** Previously reported maximum adsorption capacities of the various mineral adsorbents for Cd(II) and Pb(II) at room temperature

Adsorbent	Adsorption capacity (mg g <sup>-1</sup> )		Reference
	Cd(II)	Pb(II)	
Turkish illitic clay	13.09	53.76	4
Kaolinite	10.75	16.16	17
Montmorillonite	30.7	31.1	3
Limestone	1.3	40	27
Vermiculite	13	24	28
Wollastonite	—	0.22	29
Palygorskite	37.3	—	30
Ball clay	2.24	—	31
Sepiolite	—	51.36	32
Glauconite	4.1	—	33
Dolomite	—	19.69	34
Phosphate rock	10.46	12.78	35
Zeolite	—	155.4	36
Low-cost synthetic mineral	32.8	268.0	Present study

most other mineral adsorbents. This result reveals that LCSM has great potential for metal ions removal from contaminated water.

### 3.6. Effects of temperature and thermodynamic analysis

Thermodynamic parameters are calculated by Van't Hoff equation and presented in Table 5.  $\Delta H$  and  $\Delta S$  were calculated from the slope and intercept of the linear plot of  $\ln K_d$  versus  $1/T$  (Fig. 7). Gibbs free energy change  $\Delta G$  was calculated to be  $-4.044$ ,  $-4.182$ ,  $-4.351$  and  $-4.503$  kJ mol<sup>-1</sup> for Cd(II) adsorption and  $-4.027$ ,  $-4.318$ ,  $-4.692$  and  $-5.140$  kJ mol<sup>-1</sup> for Pb(II) adsorption at 25, 35, 45 and 55 °C, respectively. Negative value of  $\Delta G$  over the entire temperature range indicates the feasibility and spontaneity of the reaction for Cd(II) and Pb(II) removal by LCSM.<sup>37</sup> The increase of the absolute values of  $\Delta G$  with the increase of temperature (25–55 °C) suggests an increased trend in the degree of spontaneity of the metal ions sorption and high temperature is beneficial to

**Fig. 7** Plot of  $\ln K_d$  against  $1/T$  obtained for the adsorption of Cd(II) and Pb(II) onto LCSM.

adsorption of heavy metals.<sup>38,39</sup> The  $\Delta H$  parameter was found to be 0.915 and 7.014 kJ mol<sup>-1</sup> for Cd(II) and Pb(II) adsorption, respectively. The positive value of  $\Delta H$  indicates the endothermic nature of adsorption and the metal ions removal capacity increased with increasing temperature (see Fig. 6), which imply a chemical adsorption process rather than physisorption.<sup>38</sup> This results are consistent with the deduction obtained from the adsorption kinetics and free energy values from the D-A model. The  $\Delta S$  parameter was found to be 16.5 J mol<sup>-1</sup> K<sup>-1</sup> for Cd(II) adsorption and 36.9 J mol<sup>-1</sup> K<sup>-1</sup> for Pb(II) adsorption. Positive value of  $\Delta S$  for Cd(II) and Pb(II) indicates that the reaction was accompanied increased randomness at the solid-solution interface.<sup>40</sup>

### 3.7. Desorption performance

In order to prevent the heavy metal adsorbed onto LCSM released into natural water again under the impact of acid rain or acid wastewater, an advanced adsorbent for the metal ions removal should possess higher removal capability as well as better stability. Fig. 8 shows the Cd(II) and Pb(II) desorption rates with respect to solutions at varied pH values *i.e.* 3.0, 2.0, 1.0 and 0.5. It can be observed that Cd(II) and Pb(II) desorption

**Table 5** Thermodynamic parameters for the adsorption of Cd(II) and Pb(II) onto LCSM<sup>a</sup>

Metal ions	Temperature (°C)	Van't Hoff equation: <sup>37</sup> $\ln K_d = \frac{\Delta S}{R} - \frac{\Delta H}{RT}$ ; $\Delta G = -RT \ln K_d$			
		$K_d$ (cm <sup>3</sup> g <sup>-1</sup> )	$\Delta G$ (kJ mol <sup>-1</sup> )	$\Delta H$ (kJ mol <sup>-1</sup> )	$\Delta S$ (J mol <sup>-1</sup> K <sup>-1</sup> )
Cd(II)	25	5.043	-4.011	0.915	16.5
	35	5.115	-4.182		
	45	5.181	-4.351		
	55	5.210	-4.503		
Pb(II)	25	5.077	-4.027	7.014	36.9
	35	5.395	-4.318		
	45	5.894	-4.692		
	55	6.579	-5.140		

<sup>a</sup>  $K_d$  is the distribution coefficient for the removal,  $\Delta G$ ,  $\Delta S$  and  $\Delta H$  are the Gibbs free energy, entropy and enthalpy change, respectively.  $R$  is the universal gas constant (8.314 J mol<sup>-1</sup> K<sup>-1</sup>),  $T$  is the temperature (K).



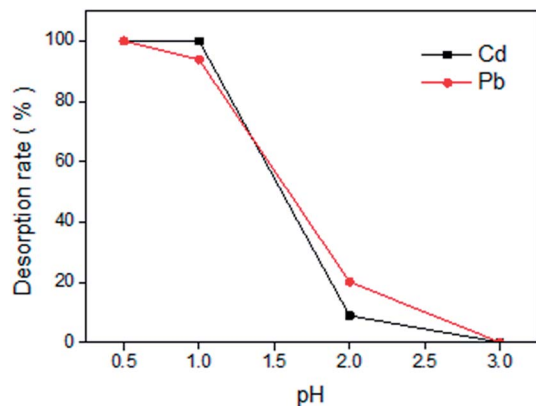


Fig. 8 Effect of pH on the desorption rates of LCSM for Cd(II) and Pb(II) at 25 °C.

rates enhanced with decreasing of pH. The adsorbed Cd(II) and Pb(II) onto LCSM can hardly be desorbed at pH 3.0 and the desorption rates were even below 20% at pH 2.0, indicating the excellent stability of LCSM and the heavy metal adsorbed can hardly be released again as the pH of natural water is typically higher than 2. But the adsorbed Cd(II) and Pb(II) can be completely desorbed at pH 1.0 and 0.5, respectively. This because the aluminosilicate of cadmium/lead precipitates or other coordination compounds can hardly exist in strong acidic solution, which indicated that LCSM had a poor regenerability because amounts of cations as well as  $\text{SiO}_4^{4-}$  in LCSM could be washed off by strong acid elutriant. However, considering the abundance of the low-cost raw materials used for preparation, good stability and amounts of mineral nutrients (see Table 1), LCSM can still be a good alternative adsorbent for removing metal ions from natural water or soil amendment used for heavy metal immobilization because of its extensive need.

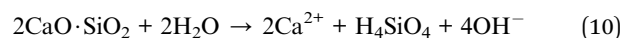
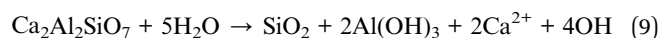
### 3.8. Mechanism of Cd(II) and Pb(II) ions removal

The SEM micrograph of the LCSM showed irregular lumps and loose aggregates with pores of different sizes and shapes (Fig. 9(A)), which was consistent with the deduction obtained from the Freundlich isotherm and H3-type hysteresis loop in the nitrogen adsorption–desorption data. Both internal and external surface of LCSM were filled off with large content of reticulation after the adsorption of Cd(II), and also with lots of

loose flocs and brachyprism after the adsorption of Pb(II). All of these new appeared shapes depositing on porous LCSM surface could be aluminosilicates of cadmium/lead complexes or other coordination compounds.

To investigate the interactions between metal ions and functional groups on LCSM, the XPS analysis of the LCSM before and after metal ions adsorption were carried out and the resultant survey spectra are given in Fig. 10. The XPS spectra show the main peaks at around 531.3, 24.7, 438.5, 347.0, 306.5, 284.5, 152.5 and 101.8 eV corresponding to O 1s, O 2s, Ca 2s, Ca 2p, Mg KLL, C 1s, Si 2s and Si 2p, respectively. The binding energies of 404.6, 411.4, 413.4, 137.7 and 142.6 eV were assigned to Cd 3d<sub>5/2</sub>, Cd 3d<sub>3/2</sub>, Pb 4d, Pb 4f<sub>7/2</sub> and Pb 4f<sub>5/2</sub>, respectively, which suggests that the Cd(II) and Pb(II) are sorbed at the surface of the LCSM by precipitation or complexation. Meanwhile, it can be observed that the intensity ratios of Mg KLL/C 1s, Ca 2s/C 1s and Ca 2p/C 1s decreased drastically, while the O 1s/C 1s, O 2s/C 1s, Si 2s/C 1s, Si 2p/C 1s, Cd 3d/C 1s and Pb 4f/C 1s increased significantly after the adsorption experiment. Therefore, it can be concluded from desorption and XPS experiments that three kinds of phenomenon namely, ion exchange, adsorption and precipitation exists for Cd(II) and Pb(II) removal by LCSM (see Scheme 1).

Ion exchange of Cd(II) and Pb(II) for  $\text{Ca}^{2+}$  and  $\text{Mg}^{2+}$  is the primary mechanism for metal ions removal as LCSM has high cation exchange capacity (see Table 1), which was attribute to the resultants such as montmorillonite and zeolites (laumontite and gismondine) in the  $\text{CaO-MgO-Al}_2\text{O}_3\text{-SiO}_2\text{-H}_2\text{O}$  system. Meanwhile, the significant difference in silicon and oxygen peaks before and after metals adsorption suggest that insoluble compounds such as aluminosilicate of cadmium/lead or hydroxide precipitates. This process can be represented by following equations:



On the other hand, heavy metals cannot precipitate below pH 4.0,<sup>41</sup> therefore, the adsorption of heavy metals in acidic solutions can be described by following equation:

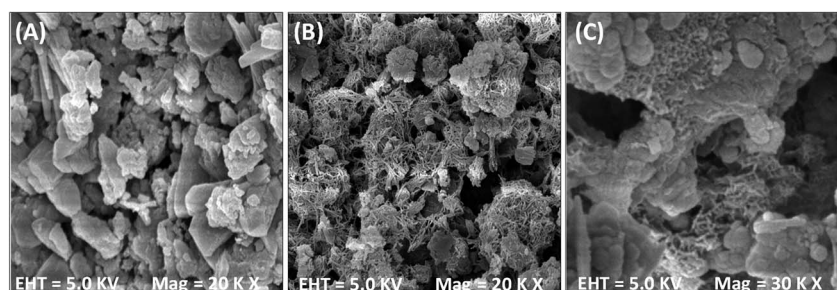


Fig. 9 The surface morphology evolution of LCSM (A), Cd(II) ion loaded LCSM (B) and Pb(II) ion loaded LCSM (C).





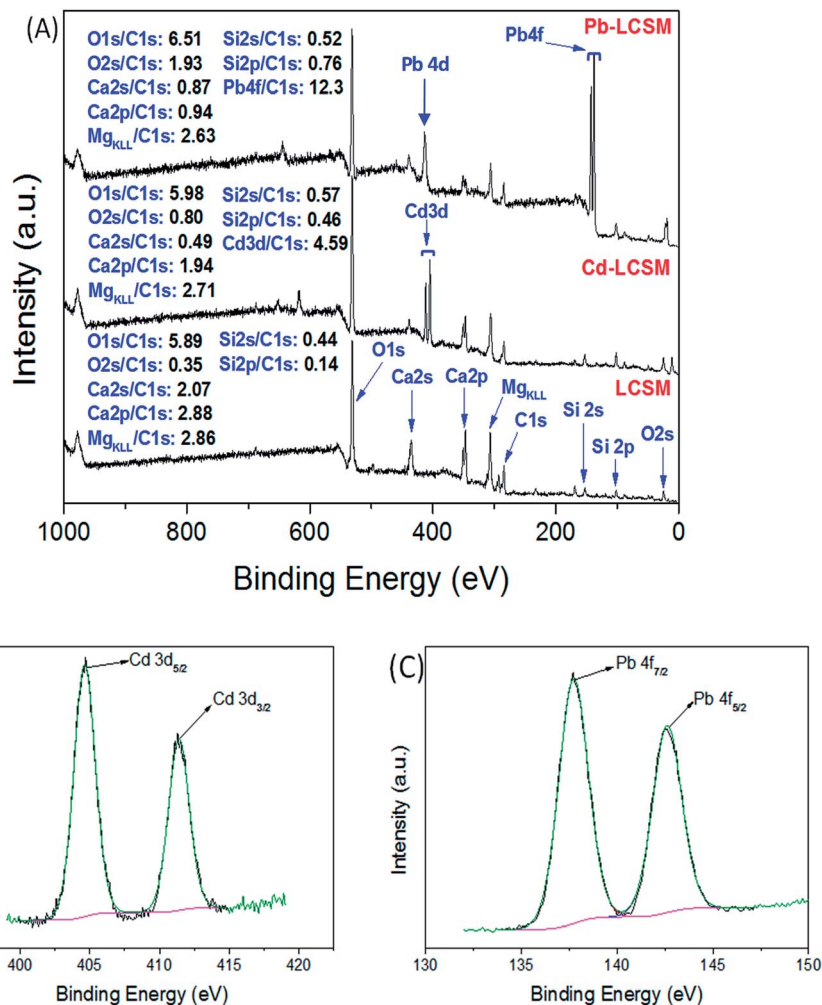
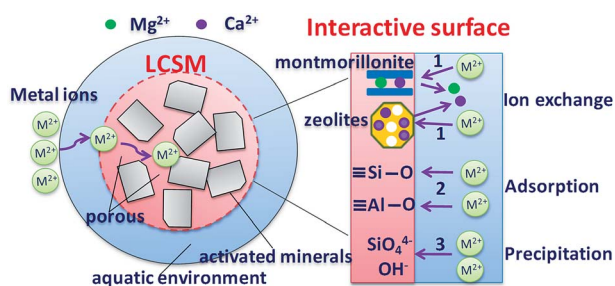
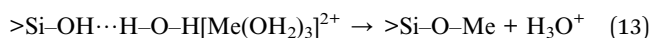


Fig. 10 XPS wide scan showing surface elemental composition of LCSM, Cd-LCSM and Pb-LCSM (A), High-resolution XPS spectra of Cd 3d (B) and Pb 4f (C) of LCSM after Cd(II) and Pb(II) adsorption.



Scheme 1 Mechanism of heavy metal ions removal by LCSM.



This process occurs due to the ionization and hydrolysis of surfaces silanol sites ( $\equiv\text{Si}-\text{OH}$ ) and aluminols ( $\equiv\text{Al}-\text{OH}$ ).<sup>42</sup> In conclusion, removal of metal ions by LCSM occurs mainly by an ion exchange mechanism, followed by precipitation and adsorption.

## 4. Conclusion

In this study, LCSM synthesized by a mixture of low-cost mineral materials under heat activation and hydration process, contains gehlenite, montmorillonite and zeolites (laumontite and gismondine), is an efficient adsorbent for the removal of Cd(II) and Pb(II) from natural water. High percentage removal of Cd(II) and Pb(II) ions were found in a wide range of pH and the adsorption process was endothermic and spontaneous, following the Freundlich isotherms. The adsorption equilibrium was attained within 30 min and the kinetic data were better fit the pseudo-second order kinetic model. It was found that the mechanism of metal removal is mainly ion exchange, followed by precipitation and adsorption. The maximum removal capacity of LCSM was 32.8 for Cd(II) and 268 mg g<sup>-1</sup> for Pb(II) ions inferred from the Freundlich model at 25 °C, which showed outstanding capabilities for the removal of Cd(II) and Pb(II) ions. LCSM also possesses excellent chemical stability and the adsorbed Cd(II) and Pb(II) onto LCSM can hardly be desorbed in natural water. Meanwhile, LCSM is rich



in available K, Ca, Mg and Si, which are essential cations for soil and crops growth. These results showed that LCSM could be a viable alternative to current costly methods of removing heavy metals from natural water or soil amendment used for heavy metal immobilization, considering its extensive need.

## Conflicts of interest

There are no conflicts to declare.

## Acknowledgements

This work was supported by the National Science and Technology Support Program (2015BAD05B05+2) and Application Project of Guangzhou Environment Protection Bureau (x2hj-B4160270) and Program Project of Guangdong Science and technology (20130323C).

## References

- 1 P. Z. Ray and H. J. Shipley, *RSC Adv.*, 2015, **5**, 29885–29907.
- 2 H. N. M. E. Mahmud, A. O. Huq and R. Binti Yahya, *RSC Adv.*, 2016, **6**, 14778–14791.
- 3 S. S. Gupta and K. G. Bhattacharyya, *J. Environ. Manag.*, 2008, **87**, 46–58.
- 4 D. Ozdes, C. Duran and H. B. Senturk, *J. Environ. Manage.*, 2011, **92**, 3082–3090.
- 5 T. A. Kurniawan, G. Y. S. Chan, W. H. Lo and S. Babel, *Chem. Eng. J.*, 2006, **118**, 83–98.
- 6 A. Sdiri, T. Higashi, T. Hatta, F. Jamoussi and N. Tase, *Chem. Eng. J.*, 2011, **172**, 37–46.
- 7 B. H. Hameed, A. T. M. Din and A. L. Ahmad, *J. Hazard. Mater.*, 2007, **141**, 819–825.
- 8 S. O. Yong, J. E. Yang, Y. S. Zhang, S. J. Kim and D. Y. Chung, *J. Hazard. Mater.*, 2007, **147**, 91.
- 9 W. Wang, G. Tian, Z. Zhang and A. Wang, *Chem. Eng. J.*, 2015, **265**, 228–238.
- 10 V. K. Jha, Y. Kameshima, K. Okada and K. J. D. Mackenzie, *Sep. Purif. Technol.*, 2004, **40**, 209–215.
- 11 M. Reinholdt, J. Miehebrendlé, L. Delmotte, R. L. Dred and M. H. Tuilier, *Clay Miner.*, 2005, **40**, 177–190.
- 12 C. A. R. O. Reyes and L. Y. V. Fiallo, *Application of Illite- and Kaolinite-Rich Clays in the Synthesis of Zeolites for Wastewater Treatment*, InTech, 2011.
- 13 V. E. D. Anjos, J. R. Rohwedder, S. Cadore, G. Abate and M. T. Grassi, *Appl. Clay Sci.*, 2014, **99**, 289–296.
- 14 L. Shi, P. Xu, K. Xie, S. Tang and Y. Li, *J. Hazard. Mater.*, 2011, **192**, 978–985.
- 15 G. Chen and L. Shi, *Clean: Soil, Air, Water*, 2016, **44**, 1690–1699.
- 16 S. Lantenois, R. Champallier, J. M. Bény and F. Muller, *Appl. Clay Sci.*, 2008, **38**, 165–178.
- 17 K. O. Adebawale, I. E. Unuabonah and B. I. Olu-Owolabi, *J. Hazard. Mater.*, 2006, **134**, 130–139.
- 18 G. Chen, K. J. Shah, L. Shi and P. C. Chiang, *Appl. Surf. Sci.*, 2017, **409**, 296–305.
- 19 S. J. Gregg and K. S. W. Sing, *Adsorption, surface area, and porosity*, Academic Pr., 1982.
- 20 A. J. Salinas, M. Valletregí, J. A. Toledofernández, R. Mendozaserna, M. Piñero, L. Esquivias, J. Ramírezcastellanos and J. M. Gonzálezcalbet, *Chem. Mater.*, 2009, **1**, 41–47.
- 21 K. S. W. Sing, *Pure Appl. Chem.*, 2009, **57**, 2201–2218.
- 22 H. Z. Mousavi, A. Hosseynifar, V. Jahed and S. A. M. Dehghani, *Braz. J. Chem. Eng.*, 2010, **27**, 454–455.
- 23 B. Preetha and T. Viruthagiri, *Afr. J. Biotechnol.*, 2005, **4**, 506–508.
- 24 I. Ghodbane and O. Hamdaoui, *J. Hazard. Mater.*, 2008, **160**, 301–309.
- 25 F. Zhang, J. Lan, Z. Zhao, Y. Yang, R. Tan and W. Song, *J. Colloid Interface Sci.*, 2012, **387**, 205–212.
- 26 V. J. Inglezakis, *Microporous Mesoporous Mater.*, 2007, **103**, 72–81.
- 27 G. Rangelporras, J. B. García magno and M. P. Gonzálezmuñoz, *Desalination*, 2010, **262**, 1–10.
- 28 G. Abate and J. C. Masini, *Colloids Surf., A*, 2005, **262**, 33–39.
- 29 K. P. Yadava, B. S. Tyagi and V. N. Singh, *J. Chem. Technol. Biotechnol.*, 1991, **51**, 47–60.
- 30 W. Wang, H. Chen and A. Wang, *Sep. Purif. Technol.*, 2007, **55**, 157–164.
- 31 V. Chantawong, N. W. Harvey and V. N. Bashkin, *Water, Air, Soil Pollut.*, 2003, **148**, 111–125.
- 32 E. Eren and H. Gumus, *Desalination*, 2011, **273**, 276–284.
- 33 E. H. Smith, W. Lu, T. Vengris and R. Binkiene, *Water Res.*, 1996, **30**, 2883–2892.
- 34 M. Irani, M. Amjadi and M. A. Mousavian, *Chem. Eng. J.*, 2011, **178**, 317–323.
- 35 Z. Elouear, J. Bouzid, N. Boujelben, M. Feki, F. Jamoussi and A. Montiel, *J. Hazard. Mater.*, 2008, **156**, 412–420.
- 36 D. Leppert, *Min. Eng.*, 1990, **42**, 604–608.
- 37 M. Xie, L. Zeng, Q. Zhang, Y. Kang, H. Xiao, Y. Peng, X. Chen and J. Luo, *J. Alloys Compd.*, 2015, **647**, 892–905.
- 38 Z. Cai, J. Jia, Q. Zhang and H. Yang, *RSC Adv.*, 2015, **5**, 82310–82323.
- 39 Y. Li, J. Liu, Q. Yuan, H. Tang, F. Yu and X. Lv, *RSC Adv.*, 2016, **6**, 45041–45048.
- 40 M. Mohapatra and S. Anand, *J. Hazard. Mater.*, 2007, **148**, 553–559.
- 41 D. H. Kim, M. C. Shin, H. D. Choi, C. I. Seo and K. Baek, *Desalination*, 2008, **223**, 283–289.
- 42 B. Sigfusson, A. A. Meharg and S. R. Gislason, *Environ. Sci. Technol.*, 2008, **42**, 8816.

